Article

Chance-Constrained Optimization Dispatch and Demand Response Control of Thermostatically Controlled Loads and Plug-in Electric Vehicles

Jianqiang Hu [1,†,‡], Jinde Cao [1,‡*]

[1] Jiangsu Provincial Key Laboratory of Networked Collective Intelligence, School of Mathematics, Southeast University, Nanjing 211189, China; jqhu@seu.edu.cn(H.J.); jdcao@seu.edu.cn(C.J.)
[2] Yonsei Frontier Lab, Yonsei University, Seoul 03722, Korea
* Correspondence: jdcao@seu.edu.cn
† School of Mathematics, Southeast University, Nanjing 211189, China
‡ These authors contributed equally to this work.

Abstract: Demand response flexible loads can provide fast regulation and ancillary services as reserve capacity in power systems. This paper proposes a joint optimization dispatch control strategy for source-load system with stochastic renewable power injection and flexible thermostatically controlled loads (TCLs) and plug-in electric vehicles (PEVs). Specifically, the optimization model is characterized by a chance constraint look-ahead programming to maximal the social welfare of both units and load agents. By solving the chance constraint optimization with sample average approximation (SAA) method, the optimal power scheduling for units and TCL/PEV agents can be obtained. Secondly, two demand response control algorithms for TCLs and PEVs are proposed respectively based on the aggregate control models of the load agents. The TCLs are controlled by its temperature setpoints and PEVs are controlled by its charging power such that the DR control objective can be fulfilled. The effectiveness of the proposed dispatch and control algorithm has been demonstrated by the simulation studies on a modified IEEE 39 bus system with a wind farm, a photovoltaic power station, two TCL agents and two PEV agents.

Keywords: Chance constraint programming; Source-load systems; Demand response control; Thermostatically controlled loads (TCLs); Plug-in electric vehicles (PEVs).

1. Introduction

With the rapid increase in energy consumption and environmental pollution, renewable energy power generation is becoming more and more popular and various kinds of distributed generations are connecting into the power grid. While the incorporation of renewable energy units give rise to the increasing need for the resource capacity or ancillary services if there exists major forecast uncertainty. Meanwhile, flexible loads in the demand side can provide different kinds of ancillary services, such as frequency regulation, load following, and some other services. A widely adopted flexible loads for these services include thermostatically controlled loads (TCLs) and plug-in electric vehicles (PEVs), which can respond the power dispatch or electricity price timely. To address these concerns, there has been lots of valuable research on the coordination and interaction of traditional units, renewable units, and flexible loads of source-load systems [1–4].

Renewable power generation has gained much attention and been in an increasing trend, which is beneficial to environment and economics. Especially, wind and photovoltaic generation are thought to be the most developed renewable sources worldwide. However, the power produced by these renewable energies largely depends on natural environmental conditions, such as wind speed or illumination intensity, which are stochastic and cannot be precisely predicted.

The uncertainty of the renewable power may pose new challenges for power system operation and control, especially during times of high penetration [5]. To provide a flexible and comprehensive consideration of the forecast error of renewable power [6], a common solution is to restrict wind power and abandon light power so as to protect the power

check for updates

Citation: Hu, J.; Cao, J. Chance-Constrained Optimization and DR Control of TCLs and PEVs. *Preprints* **2021**, *1*, 0. https://doi.org/

Received:
Accepted:
Published:

 doi:10.20944/preprints202109.0016.v1

systems. Another solution is utilizing the various optimization methods. The look-ahead dispatch method was considered in [7,8], which has been proved to be an effective strategy to reduce the power imbalance caused by the injection of renewable power [9]. By taking into account of the uncertainty of renewable power, robust optimization [10,11], stochastic optimization [12,13] and chance-constrained stochastic optimization [14,15] have been the most popular methods to account for uncertainties in power generation.

On the other hand, demand response of power grids has already switched from traditional mode of load curtailment to the mode of dynamical response without interference with users' comfort levels [16]. The DR optimization has received much attention. The authors in [17] proposed a hierarchical demand response architecture to control and coordinate the performance of various DR category resources. Demand response controllability was investigated in [18] for the unit commitment model with limited predictability and residential DR resources. By considering the site selection and the incentive price, an optimal strategy for responsive loads was proposed in [19] for source-network-load system. Online demand response for non-deferrable loads was investigated in [20] with rechargeable battery and renewable energy. By the method of the alternating direction method of multipliers, a hierarchical robust distributed optimization was proposed for demand response services [21].

As for the TCL agents, it has been shown that TCLs can provide power balancing reserves when aggregated due to their thermal energy storage capacity [22,23]. By using switching-rate actuation, the authors in [24] studied the demand response of TCLs and household refrigerators. Distributed load following was investigated in [16] for aggregate TCL loads. The authors in [25] presents a mean-field model for analysis and control for aggregate demand of heterogeneously TCLs. By using a stochastic Markov decision process and distributed robust optimization, [26] internalize the exogenous uncertain dynamics of TCLs.

Literature of demand response and EV charging scheduling has proved that EVs will become the main demand response resources in the near future. Lots of research are concentrated on the charging optimization and control problems. By designing a smart charging scheme for PEV, it has been shown in [27] that the aggregate EVs are able to reduce the peak demand or peak shaving. A fair demand response strategy for EVs was proposed in [28] for a cloud based energy management service with a given time period. The authors in [29] proposed a charging load model for an electric vehicle charging station which could be integrated to distribution systems so as to obtain the optimal charging decisions for demand response provision.

Both aggregate TCLs and aggregate PEVs are large scale flexible loads in power grids, which can be involved in the DR programme together to share the power imbalance. By considering the uncertainty in renewable energy generation, load consumption, and load reserve capacities, a chance constrained optimal power flow model was proposed in [30,31] to procure minimum cost energy. The authors in [32] proposed a chance constrained optimal power flow model to schedule power production of both generators and controllable electric loads. By the method of stochastic model predictive control, the authors in [33] investigated the optimal power dispatch and control for power grids with renewable energy resources and EVs. Based on the mixed integer linear programming method, intelligent DR for industrial energy management was designed in [34] by considering TCLs and EVs.

Motivated by the above observations, this paper intends to investigate the optimization dispatch and demand response control of source-load systems with uncertain renewable power injection and flexible TCL and PEV load agents. To the best knowledge of authors, most of the demand response problems are solved by various kinds of optimization models and methods, few published literature are concerned this problem by control algorithms. This paper will solve the demand response optimal power allocation and achievement problems of source-load systems via control models and control strategies for flexible loads. The main contributions are summarized as follows: 1) A probabilistic controllable interval is introduced to the chance-constraint look-ahead optimization, which

Preprints (www.preprints.org) | NOT PEER-REVIEWED | Posted: 1 September 2021 doi:10.20944/preprints202109.0016.v1

can cope with the uncertainty of both the renewable power generation and the flexible load response; 2) Compared with discrete-time on/off control of TCLs, a continuous-time setpoint temperature regulating control algorithm based on aggregated model is proposed to guidance the power change of the TCL agent; 3) A time-varying charging power control algorithm based on the saturation function is proposed for the PEV agent such that the aggregate PEVs can follow the reference power trajectory.

An outline of the rest paper is organized as follows. Section **??** states the problem formulation and the optimization and control framework. Section 3 provides the chance-constraint look-ahead programming model for the source-load system with the injection of renewable power and flexible TCL/PEV agents. Section 4 describes the aggregate model for TCL/PEV agents and designs the corresponding control algorithms for the optimal power profile tracking. Section 5 shows the effectiveness of the proposed optimization and control algorithm on a modified IEEE 39 bus system. Section 6 discusses the optimization and control framework and draws the conclusions.

2. Problem Formulation

Consider the coordination optimization problem of a source-load system, where the source of the system includes the traditional generating units and renewable power (mainly wind power and photovoltaic power) and the load of the system includes rigid load and flexible load. The rigid loads, such as lighting and computers, are always uncontrollable but can be predicted. The flexible loads, such as thermostatically controlled loads and plug-in electric vehicles, can be controlled by the corresponding control signals. On the other hand, the renewable power injection is always a random variable because of the wind speed and the ambient temperature and illumination are always random ones. Therefore, how to balance the power production and consumption with the maximal social welfare is a crucial problem among units and flexible loads.

This paper intends to solve this problem by setting up a chance constrained look-ahead programming model for the source-load system and designing two kinds of demand response control algorithms for TCLs and EVs. Specifically, flexible loads are aggregated as load agent which can be involved in the electricity market to participate in the load bidding. The terminal DR loads is controlled by the load agent by issuing the corresponding control signals. The schematic diagram of the optimization dispatch is shown in Fig. 1.

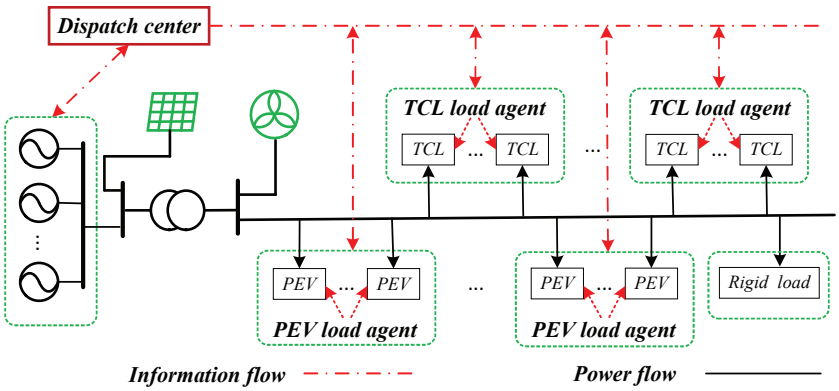

Figure 1. The structure of the optimization dispatch framework of source-load systems.

Based on the prediction of the rigid load and the actual renewable power injection and the day-ahead power generation plan, the look-ahead optimization dispatch with chance constraints can be solved by the sample average approximation (SAA) method [37,38]. Furthermore, the generating units respond optimal generating instructions and the flexible load agents achieve the optimal power profile by demand response control of massive terminal small controlled loads. The detailed control models and the control algorithms of TCL agents and PEV agents will be discussed in the following.

Preprints (www.preprints.org) | NOT PEER-REVIEWED | Posted: 1 September 2021 doi:10.20944/preprints202109.0016.v1

3. Chance Constrained Look-ahead Optimization

This paper considers the joint real-time economic dispatch problem for generating units and flexible load agents by considering the uncertainty of renewable energy power generation. The objective of the power scheduling is to maximize the social welfare, i.e., maximizing both generating units and load agents:

$$\max \sum_{t=1}^{T} \mathbb{F}(\mathcal{P}(t)) = \sum_{t=1}^{T} \Big[\sum_{i \in G} \Omega_{G,i}\big(P_{G,i}(t), p(t)\big) + \sum_{j \in L} \Omega_{L,j}\big(P_{L,j}(t), p(t)\big) \Big], \tag{1}$$

where $\mathbb{F}$ is the total social welfare with respect to the real-time power variable $\mathcal{P}(t) = [P_1(t), P_2(t), \ldots, P_{|G|+|L|}(t)]^T = \mathcal{P}_0(t) + \Delta\mathcal{P}(t)$ (day-ahead scheduling plus intra-day corrective scheduling); $p(t)$ is the time-of-use (TOU) power price; $\Omega_{G,i}(\cdot)$ and $\Omega_{L,j}(\cdot)$ are the welfare functions of the ith generating unit and the jth load agent, which are given as follows,

$$\begin{cases} \Omega_{G,i}(P_{G,i}(t), p(t)) = p(t)P_{G,i}(t) - C_i\big(P_{G,i}(t)\big), \\ \Omega_{L,j}(P_{L,j}(t), p(t)) = U_l\big(P_{L,j}(t)\big) - p(t)P_{L,j}(t). \end{cases} \tag{2}$$

For the units, the cost function $C_i(\cdot)$ usually can be approximated by a quadratic convex function $C_i(P_i) = a_i P_i^2 + b_i P_i + c_i$, where a_i, b_i and c_i are predetermined constants and P_i is the generated power. For the load agents, the utility function $U_j(\cdot)$, often assumes to be the convex utility function with the zero initial value, is a quadratic utility function which can be described by [35,36].

$$U_j(P_{L,j}) = \begin{cases} \omega_j P_{L,j} - \alpha_j P_{L,j}^2, & 0 \le P_{L,j} \le \dfrac{\omega_j}{2\alpha_j}, \\ \omega_j^2 / 4\alpha_j, & P_{L,j} \ge \dfrac{\omega_j}{2\alpha_j}, \end{cases} \tag{3}$$

where ω_j and α_j are predetermined constant coefficients.

Considering the randomness of the actual renewable power, the following chance constraint with a controllable interval is involved:

$$\Pr\Big(P_{lo} \le \sum_{i \in G} P_{G,i}(t) + P_{Rew}(t) - \sum_{j \in L} P_{L,j}(t) - P_D(t) \le P_{hi} \Big) \ge p_a, \tag{4}$$

where $[P_{lo}, P_{hi}]$ is the controllable confidence interval of the source-load system which is often set to be smaller than the actual operation interval because of the response uncertainty of the flexible DR loads; $P_{Rew}(t) = P_{wi}(t) + P_{pv}(t)$ is the renewable power injection with the random wind power variable P_{wi} and the random photovoltaic power P_{pv}; P_D is the prediction value of the rigid load in the system; the probability p_a is required at least 95%.

Other considered inequality constraint conditions for such an optimization problem are given as follows:

$$\begin{cases} P_{G,i}^{\min} \le P_{G,i}(t) \le P_{G,i}^{\max}, \\ -R_{G,i}^{\mathrm{dn}} \le \dfrac{1}{\Delta T}\big(P_{G,i}(t+1) - P_{G,i}(t)\big) \le R_{G,i}^{\mathrm{up}}, \\ P_{L,j}^{\min}(t) \le P_{L,j}(t) \le P_{L,j}^{\max}(t), \\ -R_{L,j}^{\mathrm{dn}} \le \dfrac{1}{\Delta T}\big(P_{L,j}(t+1) - P_{L,j}(t)\big) \le R_{L,j}^{\mathrm{up}}, \end{cases} \tag{5}$$

for $\forall i \in G, j \in L$ and $t = 1, \ldots, T$; $P_{G,i}^{\min}$ and $P_{G,i}^{\max}$ are the lower and upper bounds for ith generating unit; $P_{L,j}^{\min}(t)$ and $P_{L,j}^{\max}(t)$ are the time-varying lower and upper bounds for jth

Preprints (www.preprints.org) | NOT PEER-REVIEWED | Posted: 1 September 2021 doi:10.20944/preprints202109.0016.v1

load agent; $R^{\mathrm{dn}}_{G/L}$ and $R^{\mathrm{up}}_{G/L}$ are the down and upper ramping rates of the units and load agents.

By the sample average approximation method [37,38], the optimal power scheduling for units and flexible load agents can be obtained by solving the look-ahead optimization (1)-(5) with chance constraint. In the following, the design of the demand response control algorithms for the aggregate TCL agents and the PEV agents will be provided.

The power variability and uncertainty of the renewable power are handled by the probabilistic chance-constrained optimization, where the probability distributions of the wind power and the PV power are assumed to be mutually independent. Then the joint probability density function can be derived by the probability theory. Then, the sample of the renewable power can be generated by its probability distribution. The power balance constraint is transformed to be a probability confidence interval with a predefined confidence level p_a, which is able to cope with the volatility of the renewable power. On the other hand, the inherent uncertainty of flexible TCLs and PEVs is absorbed by the reserve capacity of the system, i.e., the controllable confidence interval of the optimization constraint (4) can be set smaller than the actual operation interval of the source-load system.

4. Demand Response Control of Load Agents

It is well known that both TCLs and PEVs are small loads in the power grid compared with the traditional generating units. Therefore, how to control these dispersive loads to fulfill a global optimization objective is a key problem in the implementation of the demand response control. That is, one needs to design the corresponding control strategies such that the aggregate power $P_T(t)$ of all terminal controllable loads can track the reference power trajectory $P_{ref}(t)$ optimized in the chance constrained optimization. The approximate models for aggregated TCLs and PEVs are utilized in this paper, based on which the error feedback control strategies are proposed. The following provides detailed models and control algorithms.

4.1. Aggregated TCL Model and Feedback Control

Suppose a population of homogeneous TCLs under a common control area is aggregated as a TCL agent, the aggregate power of which based on the temperature control is approximated by a bilinear system [39] as follows,

$$\begin{cases} \dot{x}_c(t) = A_c x_c(t) + B_c x_c(t) u_c(t), \\ y_c(t) = C_c x_c(t), \end{cases} \tag{6}$$

where $x_c(t) \in \mathbb{R}^Q$ is the internal state denoting the average number of off or on TCLs in each temperature subinterval of the temperature deadband; $P_T(t) = y_c(t) \in \mathbb{R}$ is the approximate aggregate power output of the TCL agent; the coefficient matrices A_c, B_c, C_c can be founded in [39], which are omitted here for space limit; $u_c(t) \in \mathbb{R}$ is an incorporated control input satisfied the constraint

$$u_c(t) = \frac{1}{CR}(\Delta\theta_a(t) - \Delta\theta_{set}(t)) - \Delta\dot{\theta}_{set}(t), \tag{7}$$

where $C[kWh/^oC]$ is the thermal capacitance and $R[^oC/kW]$ is the thermal resistance; $\Delta\theta_a(t) = \theta_a(t) - \theta_{base}$ is the deviation value between the ambient temperature $\theta_a(t)$ and the base value θ_{base}; $\Delta\theta_{set}(t) = \theta_{set}(t) - \theta^{des}_{set}$ is a bounded deviation value between the actual temperature setpoint $\theta_{set}(t)$ and preferred setpoint temperature θ^{des}_{set} for the comfort levels of customers. $\Delta\dot{\theta}_{set}$ is the changing rate of the setpoint temperature $\theta_{set}(t)$, which needs to be designed within an interval $[\bar{\alpha}_{on}, \bar{\alpha}_{off}]$ so as to make the aggregate bilinear model (6) make senses, see the detialed illustration in [40].

Preprints (www.preprints.org) | NOT PEER-REVIEWED | Posted: 1 September 2021 doi:10.20944/preprints202109.0016.v1

Parameters $\bar{\alpha}_{on}$, $\bar{\alpha}_{off}$ are functions with the independent variables θ_{base} and θ_{set}^{des}, given as

$$\begin{cases} \bar{\alpha}_{on}(\theta_{base}, \theta_{set}^{des}) = \dfrac{1}{CR}(\theta_{base} - \theta_{set}^{des} - RP_r), \\ \bar{\alpha}_{off}(\theta_{base}, \theta_{set}^{des}) = \dfrac{1}{CR}(\theta_{base} - \theta_{set}^{des}), \end{cases} \tag{8}$$

where P_r [kW] is the energy transfer rate to or from the thermal mass, which is positive for cooling TCLs.

Next, the setpoint temperature $\theta_{set}(t)$ is determined indirectly by viewing the incorporated control $u_c(t)$ as an entire variable. By the optimization calculation from the dispatch center, the optimal power profile $P_{ref}^{tcl}(t)$ for the TCL agent can be derived. The updating of control input $u_c(t)$ is proposed based on the error feedback control:

$$u_c(t) = \mu_1\big(P_{ref}^{tcl}(t) - y_c(t)\big) + \mu_2 \int_{t_0}^{t} \big(P_{ref}^{tcl}(t) - y_c(t)\big)\mathrm{d}t, \tag{9}$$

where μ_1 and μ_2 are the control gains.

While the actual temperature setpoint deviation values of TCLs can be updated by substituting (9) into (7). Furthermore, the real-time setpoint temperature $\theta_{set}(t)$ for the TCLs in the load agent can be obtained by

$$\theta_{set}(t) = \theta_{set}^{des} + \Delta\theta_{set}(t). \tag{10}$$

According to the generated setpoint temperature control signal, the temperature of each TCL changes by the following temperature regulation differential equation:

$$\frac{\mathrm{d}\theta(t)}{\mathrm{d}t} = \frac{1}{CR}\big(\theta_a(t) - \theta(t) - s(t)RP_r\big), \tag{11}$$

where $\theta(t)$ is the internal temperature of the conditioned mass. The operation state $s(t)$ is governed by the following thermostatic switching law:

$$s(t) = \begin{cases} 0, & \text{if } s(t-\tau) = 1 \,\&\, \theta(t) < \theta^{-}(t) \\ 1, & \text{if } s(t-\tau) = 0 \,\&\, \theta(t) > \theta^{+}(t) \\ s(t-\tau), & \text{otherwise} \end{cases} \tag{12}$$

where τ is the sampling period of temperature, and the lower and upper boundaries of the temperature deadband are given as:

$$\theta^{-}(t) = \theta_{set}(t) - \frac{\delta_{db}}{2}; \quad \theta^{+}(t) = \theta_{set}(t) + \frac{\delta_{db}}{2}. \tag{13}$$

The deadband of each controlled TCL is a time-varying interval $[\theta^{-}(t), \theta^{+}(t)]$, since the setpoint temperature is regulated according to the global optimization objective.

In the above aggregate model (6), the parameters of TCLs are assumed to be homogenous for model simplification. As for the heterogeneous TCLs, there are two methods to approximate the aggregate power. The first one is to utilize the averaged equivalent model with the averaged equipment parameters. The second one is to divide the heterogeneous TCLs to multiple homogeneous groups and the homogeneous TCLs are modelled by an aggregate model.

Preprints (www.preprints.org) | NOT PEER-REVIEWED | Posted: 1 September 2021 doi:10.20944/preprints202109.0016.v1

4.2. Aggregated PEV Model and Feedback Control

As for the PEV in the power grid, the SoC equation of a single PEV is always utilized to characterize the process of the power consumption:

$$SoC(k+1) = SoC(k) + \frac{\eta_e}{B_e} u_e(k) P_e^{\max} \Delta t, \tag{14}$$

where B_e denotes the battery capacity; η_e is the charging efficiency; $P_e^{\max}$ is the maximal charging power of the PEV; Δt is the sampling period of the SoC value; $u_e(k)$ is the charging ratio needed to be designed. The value of SoC is distribute in the interval $[0, 1]$, often characterized by a actual interval $[SoC_{\min}, SoC_{\max}]$, where $SoC_{\min}$ is the minimal value for the charging battery, and $SoC_{\max}$ is the objective charging state.

Suppose a population of PEVs under a common charging control area is aggregated as a PEV agent, and the aggregate charging control model of the agent is given by a transport-based load model [41]:

$$\begin{cases} \dot{x}_e(t) = A_e x_e(t) u_e(t) + \omega(t), \\ y_e(t) = C_e x_e(t) u_e(t). \end{cases} \tag{15}$$

where $x_e(t) \in \mathbb{R}^n$ is the concentration of PEVs; $u_e(t) \in [0, 1]$ is a bounded control input denoting the charging ratio relative to the maximal charging power of the PEV (the same with $u_e(t)$ in (14)); $\omega(t) \in \mathbb{R}^n$ is the disturbance of the entering/exiting PEV flow; $y_e(t)$ is the aggregate power output of the PEV agent.

In the above aggregate model, the SoC interval $[SoC_{\min}, SoC_{\max}]$ is discretized into n equal segments of length h, and $x_{ej}(t)$ denotes the concentration of PEVs in the jth segment of the PEV agent at time t. The coefficient matrixes A_e, C_e are given with

$$A_e = \frac{1}{h} \begin{bmatrix} -P_e^{\max} & 0 & \cdots & \cdots & 0 \\ P_e^{\max} & -P_e^{\max} & \cdots & \cdots & 0 \\ \vdots & \ddots & \ddots & \cdots & \vdots \\ 0 & \cdots & P_e^{\max} & -P_e^{\max} & 0 \\ 0 & \cdots & \cdots & P_e^{\max} & 0 \end{bmatrix}_{n \times n},$$

$$C_e = [P_e^{\max}, \cdots, P_e^{\max}, 0]_n, \quad h = \frac{SoC_{\max} - SoC_{\min}}{n}.$$

Furthermore, the transport-based flow $\omega(t)$ of PEVs is defined as:

$$\omega(t) = \begin{cases} \vartheta_i f_{\text{in}}^{(i)}(t), & i = 1, 2, \ldots, n_1, \\ \vartheta_i f_{\text{in}}^{(i)}(t) - f_{\text{out}}^{(i)}(t), & i = n_1 + 1, \ldots, n, \end{cases} \tag{16}$$

where ϑ_i is the transport flow coefficient satisfying $\sum_{i=1}^{n} \vartheta_i = 1$; $f_{\text{in}}^{(i)}(t)$ is the input flow; $f_{\text{out}}^{(i)}(t)$ is the output flow at ith discretization segments ($n_1 \leq i \leq n$ governed by the transport dynamics of PEVs, given by

$$f_{\text{out}}^{(i)}(t) = f_{\text{depa}}^{(i)}(t) - f_{\text{stay}}^{(i)}(t) = \frac{P_e^{\max}}{h} x_i(t) u_e(t) - f_{\text{stay}}^{(i)}(t), \tag{17}$$

where $f_{\text{stay}}^{(i)}(t)$ means the EVs charged that can leave (the concentration of this kind of PEV load is denoted by $f_{\text{depa}}^{(i)}(t)$) while choosing not to leave at this time, such as $f_{\text{stay}}^{(i)}(t) = 0.8 f_{\text{depa}}^{(i)}(t)$ denotes 80% EVs stopped charging while waiting to leave.

The dynamic characteristic of flexible terminal EV loads is described by the variable of the transport-based flow $\omega(t)$ of PEVs, where EVs can leave the power grid with a satisfied charging objective, i.e. they do not wait to leave until the fully charged.

Preprints (www.preprints.org) | NOT PEER-REVIEWED | Posted: 1 September 2021 doi:10.20944/preprints202109.0016.v1

By the optimization calculation from the dispatch center, the optimal power profile $P_{ref}^{pev}(t)$ for the PEV agent can be derived. The updating of control input $u_e(t)$ is proposed based on the error feedback control:

$$\dot{u}_e(t) = \kappa \mathrm{sat}\big(P_{ref}^{pev}(t) - y_e(t)\big), \tag{18}$$

where κ is positive control gain; the function $\mathrm{sat}(\cdot)$ is a saturation function defined by

$$\mathrm{sat}(v) = \begin{cases} 1, & v > \epsilon \\ v/\epsilon, & -\epsilon \le v \le \epsilon \\ -1, & v < \epsilon \end{cases} \tag{19}$$

where $1/\epsilon$ is the slope of the saturation function predefined. The initial value for the reference control input is set to satisfy the constraint $0 \le u_e(0) \le 1$.

Finally, the practice charging power of PEV is $P_i(t) = P_{e,i}^{\max} u_e(t)$, then the charging state is measured by the SoC equation (14). Instead, the power capacity available for the aggregator can be calculated approximatively by the concentration of PEVs in each SoC subinterval:

$$\Delta P(t) = \sum_{j=1}^{n} x_{ej}(t) \times P_e^{\max}, \tag{20}$$

and the minimal charging time $t_j^{\min}$ for EVs in the jth segment (i.e., minimal available control period) can be calculated by

$$t_j^{\min} = \frac{B_e\big(SoC_{\mathrm{obj}} - j(SoC_{\max} - SoC_{\min})/n\big)}{\eta_e P_e^{\max}}, \tag{21}$$

and the maximal available control period $t_j^{\max} = t_j^{\mathrm{dep}} - t_j^{\mathrm{arr}}$, where t_j^{arr} and t_j^{dep} are the arrive time and the temperature time.

Meanwhile, if the dwell time of the EV is smaller than the minimal charging time, i.e.,

$$t_j^{\mathrm{dep}} - t_j^{\mathrm{arr}} < \frac{B_e\big(SoC_{\mathrm{obj}} - SoC_{\mathrm{ini}}\big)}{\eta_e P_e^{\max}}, \tag{22}$$

where SoC_{obj} and SoC_i^{ini} are the objective and the initial SoC values, then the EV is not available for scheduling, which can be viewed as disturbance for the aggregate model and its practice charging power can be set $P_i(t) = P_{e,i}^{\max}$ directly.

As for the PEV agents, the maximal and minimal regulation capacities are time-varying according to the changing of the transport flow of EVs and the states of the SoC equation. Therefore, the constraints for PEV agents is time-varying as well.

The battery of the PEV can be charged at rated power or maximal charging power by time-controlled charge scheduling to get full charged. Meanwhile, the charging power P_c of PEV can be varied in $[P_c^{\min}, P_c^{\max}]$ by turning the charging modes with the constant voltage or current. Therefore, the voltage controller or current controller can be utilized to realize the optimal charging power by $P_c = U_c \times I_c$. Such as in the voltage stabilization mode, the charging current can be controlled in the interval $[I_c^{\min}, I_c^{\max}]$ by feedback control to regulate the actual charging power. Fast charging technology for batteries have already been applied in practice to reduce charging time by increasing the charging current. On the other hand, the time-varying charging power utilized in practice is sampled with a fixed sampling period instead of the fast-changing continuous power and in each charging period, the charging power is a constant charging power as well. In order to illustrate the

Preprints (www.preprints.org) | NOT PEER-REVIEWED | Posted: 1 September 2021 doi:10.20944/preprints202109.0016.v1

accuracy of the demand response control, the relative errors are utilized to measure the control performance:

$$E_1(t) = \frac{|P_{ref}^{tcl}(t) - y_c(t)|}{P_{ref}^{tcl}(t)}, \qquad E_2(t) = \frac{|P_{ref}^{pev}(t) - y_e(t)|}{P_{ref}^{pev}(t)}. \tag{23}$$

If the optimal power tracking errors are acceptable, then the proposed demand response control algorithms can be utilized for the demand response applications.

The aggregate models of TCLs and PEVs are utilized in this paper mainly due to the fact that the actual TCL and PEV are often integrated into the power grid without extra electricity supervision. Therefore the actual aggregate power is difficult to be measured, and the aggregate models provide an approximate estimation for the aggregate power. The error feedback control algorithms are based on the tracking error of the optimal power profiles, which could ensure the tracking performance. The power response of the TCL agent is based on the temperature setpoint control signals and the power response of the PEV agent is based on the changing of charging power.

5. Case Study

This section validates the performance of the proposed chance constrained optimization and demand response control architecture through numerical simulation on a modified IEEE 39-bus test system, the unifilar diagram system structure is given in Fig. 2. Suppose that the loads under bus nodes B11, B23, B28, B32 are flexible controllable loads which are managed by the corresponding load agents TCL/PEV A1/2 and loads under the bus nodes B27 and B29 are fixed loads. On the other hand, the generators G1 $\sim$ G6 are slow units and generators G7 $\sim$ G10 are AGC units.

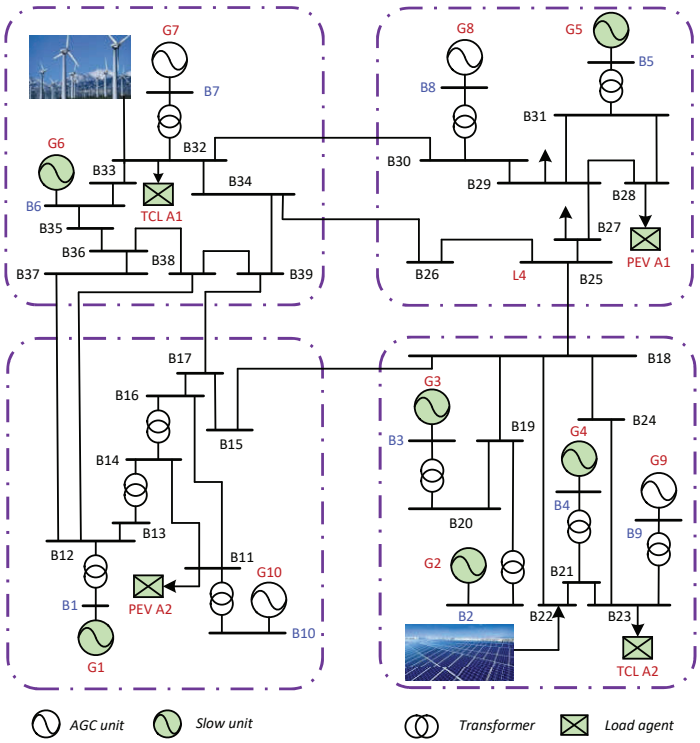

Figure 2. The modified IEEE39 bus system for testing and verification.

The flexible controllable loads serve as demand side resources, which can provide active power regulation service together with generation units. Six slow units and the four flexible load agents are dispatched by the dispatch center based on the chance constraint look-ahead dispatch, the cost coefficients and capacities for all the participants are given in Tabs. 1. We consider the optimization dispatch and demand response control of a

Preprints (www.preprints.org) | NOT PEER-REVIEWED | Posted: 1 September 2021 doi:10.20944/preprints202109.0016.v1

summer working day, where the TCLs (mainly air conditioners) and PEVs are controlled in real-time.

Table 1: Parameters of generation units and demand agents.

	Generation unit parameters (MW)					
G	a_i	b_i	$R^{\mathrm{dn}}_{G,i}$	$R^{\mathrm{up}}_{G,i}$	$P^{\min}_{G,i}$	$P^{\max}_{G,i}$
G1	0.0451	2.8213	15	20	25	200
G2	0.0365	2.2421	22	24	20	180
G3	0.0274	3.1518	20	25	30	200
G4	0.0518	2.8523	18	12	30	150
G5	0.0818	4.1533	20	16	20	200
G6	0.0353	2.3472	15	15	20	160
	Demand agent parameters (MW)					
L	α_j	ω_j	$R^{\mathrm{dn}}_{L,j}$	$R^{\mathrm{up}}_{L,j}$	$P^{\min}_{L,j}$	$P^{\max}_{L,j}$
TCL A1	0.2116	21.1621	4	6	10	50
TCL A2	0.2452	19.6168	5	9	15	40
PEV A1	0.2021	18.1892	8	6	10	45
PEV A2	0.2456	24.2234	5	7	12	50

Furthermore, the optimization period is 15 min and the look-ahead period $T = 4$; the DR control sampling period for real-time control is 20 sec. The coupling time-scale relationship is given in Fig. 3.

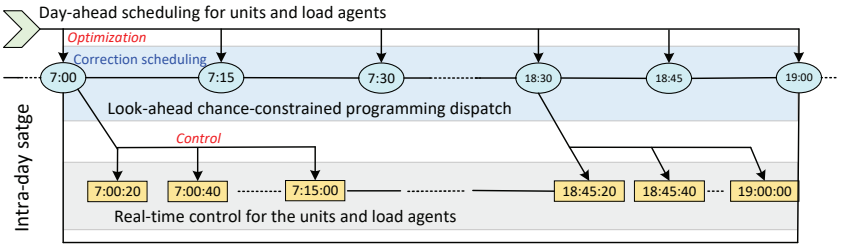

Figure 3. The time scale for the chance-constrained look-ahead programming and the real-time DR control.

In the test system, we assume all TCLs in a same agent are homogeneous, that is with the same thermal capacitance C, thermal resistance R, output cooling energy P_r, energy's transmission efficiency η, and preferred setpoint θ^{des}_{set}. The number of TCLs in each agent, and the initial proportion of the off TCLs pr_{off} and other parameters are given in Tab. 2. Suppose the ambient temperature is $24 \sim 38^oC$ given in Fig. 4 and $\theta_{base} = 34^oC$. The predicted rigid load and the TOU price are provided in Fig. 4 as well.

Table 2: TCL agents' private parameters.

Ag.	N_L	pr_{off}	R	C	P_r	η	θ^{des}_{set}	δ_{db}
A1	11780	0.52	5.12	8.82	19.63	2.92	23.15	1
A2	9730	0.49	5.44	9.89	16.56	2.71	22.45	1

On the other hand, the renewable power includes wind power and photovoltaic power, where the wind power is a random variable bounded by its rated output power. Suppose there are 50 wind generators in the wind farm with a rated power $1.5MW$ for each generator and 60 photovoltaic panels in the system. The photovoltaic power is closed related to the ambient temperature and illumination, the value is provided in Fig. 4 as well. In the simulation, the wind power and photovoltaic power are mixed together and the renewable power interval is shown in Fig. 5, and a sampled wind power curve is distributed in the power interval.

 doi:10.20944/preprints202109.0016.v1

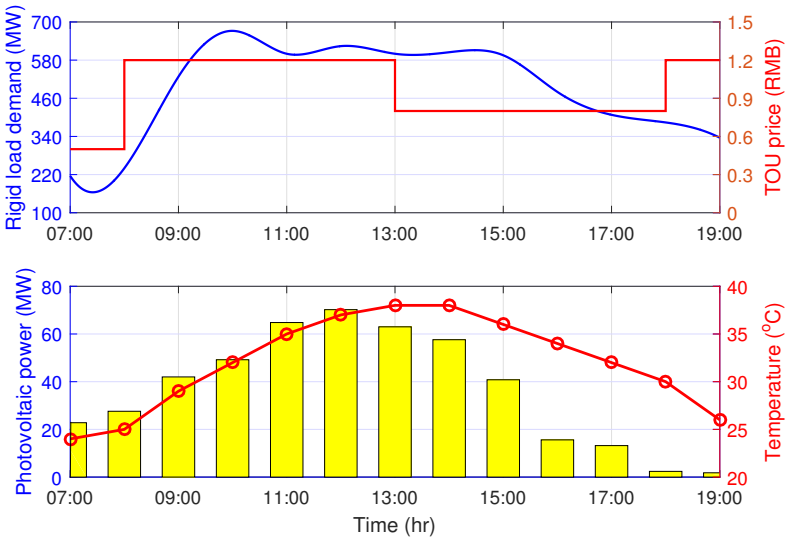

Figure 4. Load prediction and photovoltaic power injection.

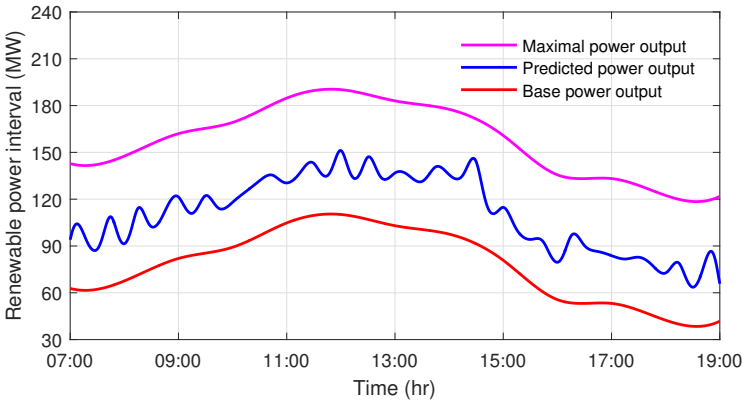

Figure 5. Renewable power interval with the stochastic wind power.

Preprints (www.preprints.org) | NOT PEER-REVIEWED | Posted: 1 September 2021 doi:10.20944/preprints202109.0016.v1

The controllable interval of the source-load system is set to be 60% of the maximal regulation capacity 100 MW, $[P_{lo}, P_{hi}] = [-60, 60]$ MW and the chance constraint probability $p_a = 95\%$. By solving the chance constraint look-ahead optimization, the optimal power trajectories for units and load agents are given in Figs. 6-7 respectively.

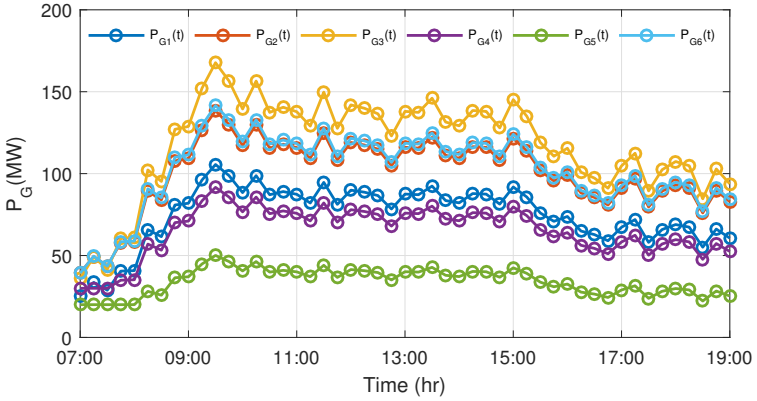

Figure 6. The optimal power output of generating units.

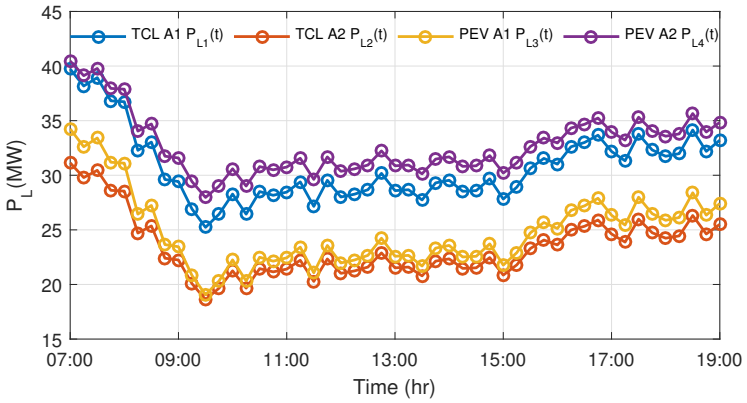

Figure 7. The optimal power consumption of load agents.

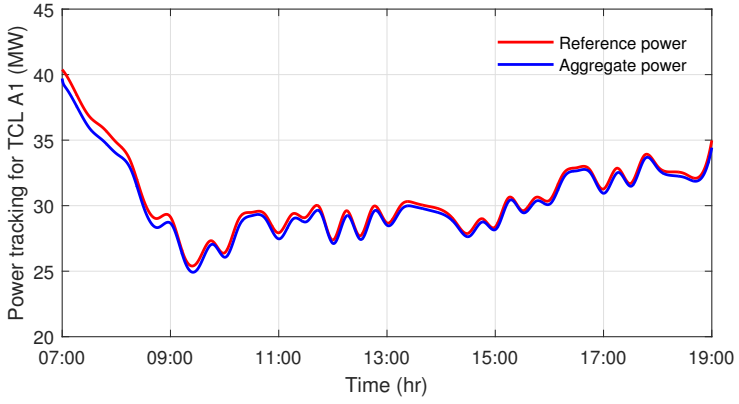

Figure 8. The power tracking of the first TCL agent.

As can be seen from Figs. 6 and 7, the power generation follows the load fluctuation and load agents gain the corresponding regulation capacity as well. If all the TCLs and PEVs are not involved in the demand response programme, then the extra power generation will be compensated by the generating units. Next, the simulation of the demand response control is illustrated.

As for the TCL agents, the state space dimension $Q = 30$, the sampling period τ is set to be 20 second and the initial temperature of the TCLs follows an uniform distribution

Preprints (www.preprints.org) | NOT PEER-REVIEWED | Posted: 1 September 2021 doi:10.20944/preprints202109.0016.v1

U$[22,25]^oC$; and the comfort temperature intervals for the two agents are given with $[21.15, 26.15]$ and $[22.45, 27.25]$ separately. By setting $\mu_1 = 0.7$ and $\mu_2 = 0.1$, and running the system (6) with control input (9), the reference power and the actual aggregate power are given in Figs. 8 and 9. The relative error curves are provided in Fig. 10, which are smaller than 0.07%.

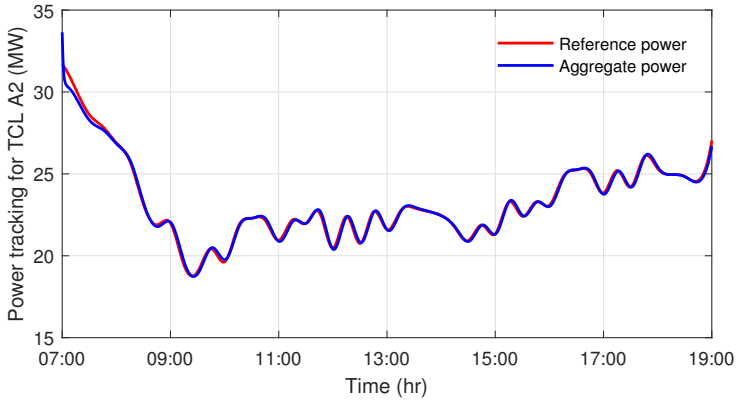

Figure 9. The power tracking of the second TCL agent.

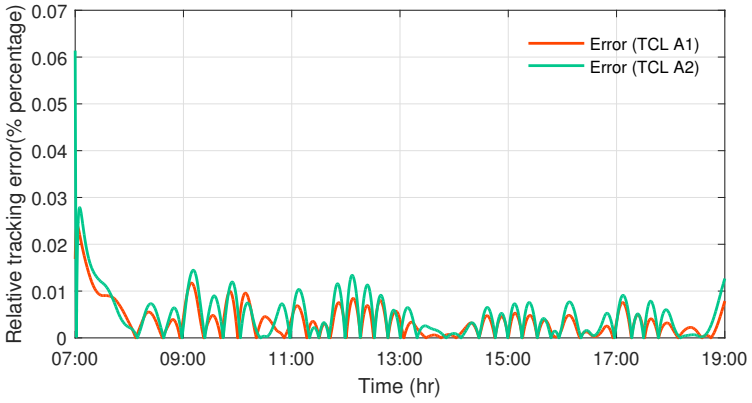

Figure 10. The relative power tracking errors of TCL agents.

As for the PEV agents, the SoC interval is set to be $[SoC_{\min}, SoC_{\max}] = [0.1, 1]$, and the interval was divided into $n = 9$ subintervals. Furthermore, $n_1 = 3$ means the EVs with the SoC value lower than 40% can only enter but not exit and EVs with the SoC value upper than 40% can enter or exit freely. The sampling period $\delta t = 20$ second as well. The initial centralization of PEV $x_{\cdot 1}(0) = [23520, 30225]$ and $x_{\cdot j}(0) = [0, 0]$ for $2 \leq j \leq n$. The hourly transport flows for the incoming EVs of two PEV agents in time period from $7:00$ to $19:00$ are given in Fig. 11. According to the survey of the daily trip lengths, over 40% of the PEVs return to the first SoC discretization segment and the transport flow coefficient θ_j is set to be $\theta_{\cdot 1} = [0.42, 0.45]$ and $\theta_{\cdot j} \in U[0.03, 0.09]$ for $2 \leq j \leq n$.

The output transport flow of PEVs can be calculated by Eq.(17), where $f^{(i)}_{\text{stay}}(t)$ is set to be $0.8 f^{(i)}_{\text{depa}}(t)$, that is 80% PEVs charged that can leave while choosing not to leave at this time. Here, $f^{(i)}_{\text{depa}}(t)$ denotes the concentration of PEV whose SoC has reached the target charging area.

By setting $\epsilon = 2$ in the saturation function and $\kappa = 0.6$, and the initial value $u_{\text{ref}}(0) = [0.372, 0.348]$ in the controller. Then by system (15) with the control input (18), the optimal power profile and aggregate power of PEV agent are given in Fig. 12 and 13 for agent PEV $A1$ and $A2$.

As can be seen from Figs. 12 and 13, the PEV agents follow the optimal charging

Preprints (www.preprints.org) | NOT PEER-REVIEWED | Posted: 1 September 2021 doi:10.20944/preprints202109.0016.v1

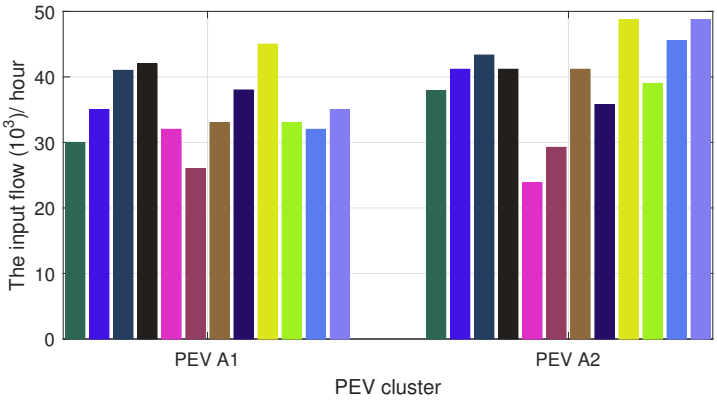

Figure 11. The input flow of each PEV cluster for hourly data.

power profile pretty well since the maximal charging power of the transport flow of PEVs in the simulation much larger than its actual charging power. The relative error curves are provided in Fig. 14, which are smaller than 0.03%.

Finally, the total response deviation curve $\Delta P = \sum_{i\in G} P_{G,i}(t) + P_{Rew}(t) - \sum_{j\in L} P_{L,j}(t) - P_D(t)$ is shown in Fig. 15. As can be seen from the figure, the deviation is distributed in the regulation interval and the statistical probability is 97.5%, which satisfies the chance constraint probability.

As can be seen from the simulation results and the relative tracking errors, the demand response control performance of the TCL and PEV agents is acceptable as long as the optimal power curves are solvable, which shows that the proposed demand response control algorithm can realize the demand response power tracking of flexible load agents. By participating in the demand response program, the owner of the TCL or PEV can get some compensation with a lower electricity costs. The proposed dispatch and control framework can be applied not only in bulk power systems but also in microgrids since the designing structure is similar.

In the upper layer of optimization calculation, the renewable power curve for 15 min's data is derived by the cubic spline interpolation method. In the lower layer of control procedure, the control interval (20s) for the flexible TCL and PEV loads is much smaller than the renewable power injection sampling period (1h), which enable the DR loads have sufficient time to track the uncertainty of the power injection.

6. Discussions and Conclusions

Compared with the traditional mode of power generation following load, the renewable power injection and the flexible loads in the demand side could participate the interactive operation of power grids. The chance constraint look-ahead optimization and demand response control algorithm proposed in this paper is effective for the coordinating operation of the source-load system, which can be applied in practice.

1) Implementation: In the proposed dispatch optimization and control framework, units and load agents report their basic information to the dispatch center and then the optimization can be solved in the dispatch center. The optimal dispatch planning is returned to the units and agents, and the units achieve the scheduled power by their own control algorithms. As for load agents, the control system of agents are equipped with the aggregate models for TCLs and PEVs, based on the error feedback algorithms, the corresponding control signals for the terminal TCLs and PEVs are generated and then broadcast to them in a centralized way. The controllable power interval can be fulfilled by AGC units and flexible loads with price compensation. In order to protect the power grid, the power interval for the optimization calculation can be set conservatively, such as 60% of the actual regulation capacity.

Preprints (www.preprints.org) | NOT PEER-REVIEWED | Posted: 1 September 2021 doi:10.20944/preprints202109.0016.v1

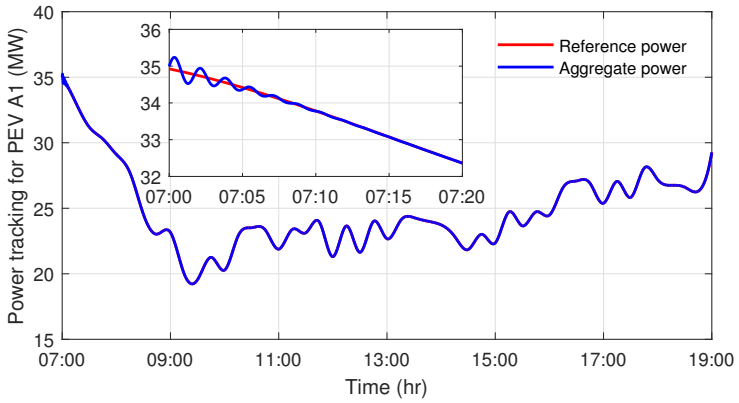

Figure 12. The power tracking of the first PEV agent.

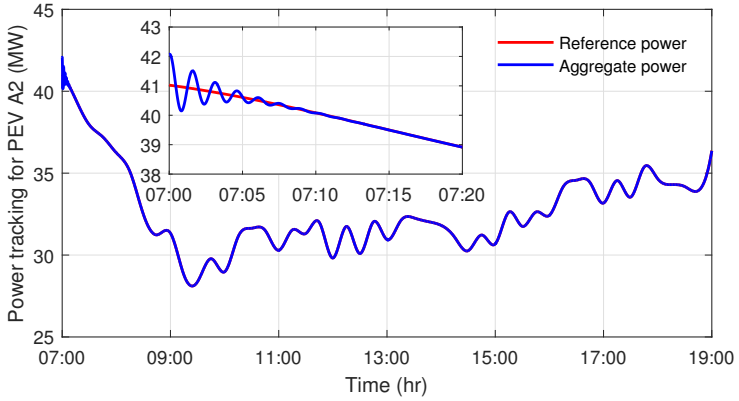

Figure 13. The power tracking of the second PEV agent.

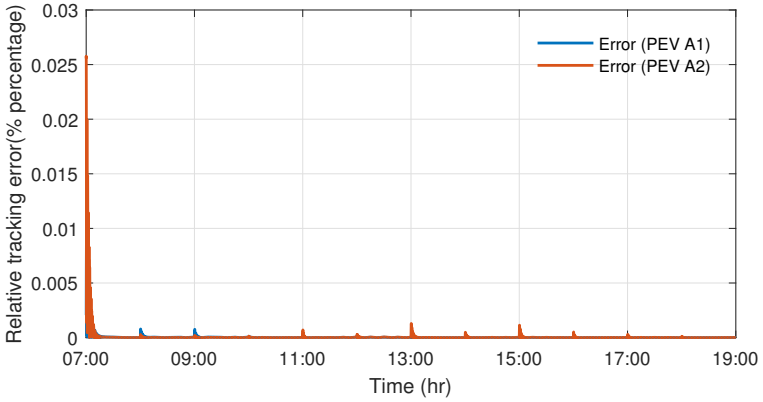

Figure 14. The relative power tracking errors of PEV agents.

 doi:10.20944/preprints202109.0016.v1

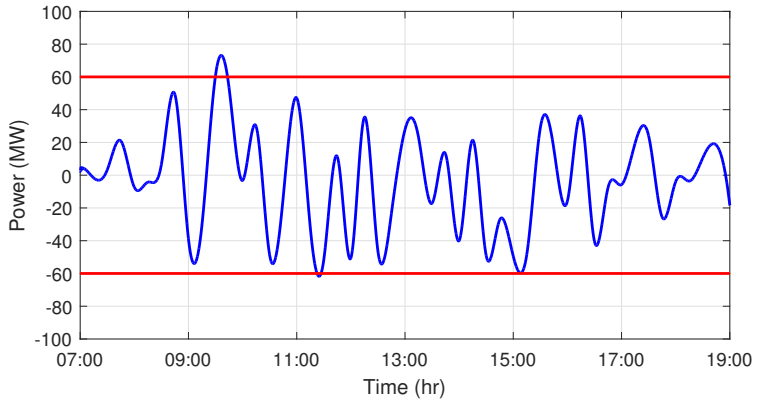

Figure 15. The stochastic response curve within the controllable confidence interval $[-60, 60]$ MW.

2) Drawbacks: As for the chance constraint optimization, there may be no optimal solution for the optimization. The confidence interval can be set larger and the confidence probability can be set smaller in the actual optimization even when there is no solution for the optimization. On the other hand, since the aggregate models are approximate models, the actual control response errors are unavoidable. It has been shown in literature that the accuracy of the model is related to the dimension of the state space model, i.e., the higher the dimensionality of the model, the higher the accuracy of the model. Conversely, the higher the dimensionality of the model, the higher the computation complexity. Therefore, a moderate choice for the dimension is feasible for the actual application. Meanwhile, since the proposed demand response control algorithm for PEVs is based on the time-varying charging power instead of on/off charging control, the EVs are assumed to be always available. Therefore, the chargeability of the EVs and user comfort levels have not be considered sufficiently in the manuscript. If the EV needs to be charged to the desired SoC with the desired minimal time instant, then the EV can be charged at the maximal charging power directly.

3) Conclusions: This paper proposed a chance constraint look-ahead optimization and demand response control framework for the source-load system. The structure ensures the load agents in the demand response program can coordinate with generating units such that the power balance could be shared together. By the aggregate models for TCL and PEV agents, the corresponding error feedback demand response control algorithms are proposed so as to generate the control signals for the terminal small loads. It has been demonstrated that the TCLs and PEVs respond well according to the proposed algorithm and the tracking errors are acceptable.

Funding: This work was supported in part by the National Key Research and Development Program of China under Grant 2018AAA0100202, in part by the National Nature Science Foundation of China under Grants 61703095, 51977032, 61833005; in part by the Natural Science Foundation of Jiangsu Province of China under Grant BK20170697, in part by the Jiangsu Provincial Key Laboratory of Networked Collective Intelligence under Grant No. BM2017002.

Conflicts of Interest: The authors declare no conflict of interest.

References

1. J. Hu, J. Cao, and T. Yong. Multi-level dispatch control architecture for power systems with demand-side resources. *IET Generation, Transmission & Distribution*, 9(16):2799–2810, 2015.
2. W. Bukhsh, C. Zhang, and P. Pinson. An integrated multiperiod OPF model with demand response and renewable generation uncertainty. *IEEE Transactions on Smart Grid*, 7(3):1495–1503, 2016.
3. J. Hu, J. Cao, J.M. Guerrero, T. Yong, and J. Yu. Improving frequency stability based on distributed control of multiple load aggregators. *IEEE Transactions on Smart Grid*, 8(4):1553–1567, 2017.

4. X. Shi, G. Wen, J. Cao, and X. Yu. Model predictive power dispatch and control with price-elastic load in energy internet. *IEEE Transactions on Industrial Informatics*, 15(3):1775–1787, 2019.
5. Z. Chen. Wind power in modern power systems. *Journal of Modern Power Systems and Clean Energy*, 1(1):2–13, 2013.
6. J.Yin and D. Zhao. Economic dispatch coordinated with information granule chance constraint goal programming under the manifold uncertainties. *IET Renewable Power Generation*, 13(8):1329–1337, 2019.
7. Y. Gu and L. Xie. Stochastic look-ahead economic dispatch with variable generation resources. *IEEE Transactions on Power Systems*, 32(1):17–29, 2017.
8. M. Javadi, T. Amraee, and F. Capitanescu. Look ahead dynamic security-constrained economic dispatch considering frequency stability and smart loads. *International Journal of Electrical Power and Energy Systems*, 108:240–251, 2019.
9. W. Wu, J. Chen, B. Zhang, and H. Sun. A robust wind power optimization method for look-ahead power dispatch. *IEEE Transactions on Sustainable Energy*, 5(2):507–515, 2014.
10. P. Xiong, P. Jirutitijaroen, and C. Singh. A distributionally robust optimization model for unit commitment considering uncertain wind power generation. *IEEE Transactions on Power Systems*, 32(1):39–49, 2017.
11. M.R. Ebrahimi and N. Amjady. Adaptive robust optimization framework for day-ahead microgrid scheduling. *International Journal of Electrical Power and Energy Systems*, 107:213–223, 2019.
12. H. Gangammanavar, S. Sen, and V.M. Zavala. Stochastic optimization of sub-hourly economic dispatch with wind energy. *IEEE Transactions on Power Systems*, 31(2):949–959, 2016.
13. S. Wang, H. Gangammanavar, S.D. Eksioglu, and S.J. Mason. Stochastic optimization for energy management in power systems with multiple microgrids. *IEEE Transactions on Smart Grid*, 10(1):1068–1079, 2019.
14. L. Yao, X. Wang, Y. Li, C. Duan and X. Wu. Distributionally robust chance-constrained AC-OPF for integrating wind energy through multi-terminal VSC-HVDC. *IEEE Transactions on Sustainable Energy*, 11(3):1414–1426, 2020.
15. M. Shahidehpour, F. Qi, F. Wen, C. Shao and Z. Li. A chance-constrained decentralized operation of multi-area integrated electricity-natural gas systems with variable wind and solar energy. *IEEE Transactions on Sustainable Energy*, 11(4): 2230–2240, 2020.
16. J. Hu, J. Cao, T. Yong, J.M. Guerrero, M.Z.Q. Chen, and Y. Li. Demand response load following of source and load systems. *IEEE Transactions on Control Systems and Technology*, 25(5):1586–1598, 2017.
17. B.P. Bhattarai, M. Levesque, B. Bakjensen, J.R. Pillai, M. Maier, D. Tipper, and K.S. Myers. Design and cosimulation of hierarchical architecture for demand response control and coordination. *IEEE Transactions on Industrial Informatics*, 13(4):1806–1816, 2017.
18. K. Bruninx, Y. Dvorkin, E. Delarue, W. Dhaeseleer, and D.S. Kirschen. Valuing demand response controllability via chance constrained programming. *IEEE Transactions on Sustainable Energy*, 9(1):178–187, 2018.
19. X. Kong, C. Yong, C. Wang, Y. Chen, and L. Yu. Optimal strategy of active distribution network considering source-network-load. *IET Generation Transmission and Distribution*, 13(24):5586–5596, 2019.
20. J. Leithon, T.J. Lim, and S. Sun. Online demand response strategies for non-deferrable loads with renewable energy. *IEEE Transactions on Smart Grid*, 9(5):5227–5235, 2018.
21. D. Michael, P. Florian, and M. Antonello. Hierarchical distributed robust optimization for demand response services. *IEEE Transactions on Smart Grid*, 9(6):6018–6029, 2018.
22. E. Vrettos and G. Andersson. Scheduling and provision of secondary frequency reserves by aggregations of commercial buildings. *IEEE Transactions on Sustainable Energy*, 7(2):850–864, 2016.
23. L. Herre, J.L. Mathieu, L. and Soder. Impact of market timing on the profit of a risk-averse load aggregator. *IEEE Transactions on Power Systems*, 35(5):3970–3980, 2020.
24. L.C. Totu, R. Wisniewski, and J. Leth. Demand response of a TCL population using switching-rate actuation. *IEEE Transactions on Control Systems and Technology*, 25(5):1537–1551, 2017.
25. N.Mahdavi and J.H. Braslavsky. Modelling and control of ensembles of variable-speed air conditioning loads for demand response. *IEEE Transactions on Smart Grid*, 11(5):4249–4260, 2020.
26. A. Hassan, R. Mieth, D. Deka, and Y. Dvorkin. Stochastic and distributionally robust load ensemble control. *IEEE Transactions on Power Systems*, 35(6): 4678–4688, 2020.

27. G. Zhang, S.T. Tan, and G.G. Wang. Real-time smart charging of electric vehicles for demand charge reduction at non-residential sites. *IEEE Transactions on Smart Grid*, 9(5):4027–4037, 2018.
28. Y. Chen and J.M. Chang. Fair demand response with electric vehicles for the cloud based energy management service. *IEEE Transactions on Smart Grid*, 9(1):458–468, 2018.
29. O. Hafez and K. Bhattacharya. Integrating EV charging stations as smart loads for demand response provisions in distribution systems. *IEEE Transactions on Smart Grid*, 9(2):1096–1106, 2018.
30. Y. Zhang, S. Shen, and J.L. Mathieu. Distributionally robust chance-constrained optimal power flow with uncertain renewables and uncertain reserves provided by loads. *IEEE Transactions on Power Systems*, 32(2):1378–1388, 2017.
31. X. Fang, B. Hodge, E. Du, C. Kang, and F. Li. Introducing uncertainty components in locational marginal prices for pricing wind power and load uncertainties. *IEEE Transactions on Power Systems*, 34(3):2013–2024, 2019.
32. M. Vrakopoulou, B. Li, and J.L. Mathieu. Chance constrained reserve scheduling using uncertain controllable loads part I: Formulation and scenario-based analysis. *IEEE Transactions on Smart Grid*, 10(2):1608–1617, 2019.
33. B. Wang, P. Dehghanian, and D. Zhao. Chance-constrained energy management system for power grids with high proliferation of renewables and electric vehicles. *IEEE Transactions on Smart Grid*, 11(2):2324–2336, 2020.
34. J. Wang, Y. Shi, and Y. Zhou. Intelligent demand response for industrial energy management considering thermostatically controlled loads and EVs. *IEEE Transactions on Industrial Informatics*, 15(6):3432–3442, 2019.
35. P. Samadi, H. Mohsenian-Rad, R. Schober, and V.W.S. Wong. Advanced demand side management for the future smart grid using mechanism design. *IEEE Transactions on Smart Grid*, 3(3):1170–1180, 2012.
36. N. Rahbari-Asr, U. Ojha, Z. Zhang, and M.-Y. Chow. Incremental welfare consensus algorithm for cooperative distributed generation/demand response in smart grid. *IEEE Transactions on Smart Grid*, 5(6):2836–2845, 2014.
37. A.J. Kleywegt, A. Shapiro, and T. Homemdemello. The sample average approximation method for stochastic discrete optimization. *SIAM Journal on Optimization*, 12(2):479–502, 2002.
38. X. Zhou, X. Wang, T. Huang, and C. Yang. Hybrid intelligence assisted sample average approximation method for chance constrained dynamic optimization. *IEEE Transactions on Industrial Informatics*, 17(9):6409–6418, 2021.
39. J. Hu, J. Cao, M.Z.Q. Chen, J. Yu, J. Yao, S. Yang, and T. Yong. Load following of multiple heterogeneous TCL aggregators by centralized control. *IEEE Transactions on Power Systems*, 32(4):3157–3167, 2017.
40. S. Bashash and H.K. Fathy. Modeling and control of aggregate air conditioning loads for robust renewable power management. *IEEE Transactions on Control Systems Technology*, 21(4):1318–1327, 2013.
41. S. Bashash and H.K. Fathy. Transport-based load modeling and sliding mode control of plug-in electric vehicles for robust renewable power tracking. *IEEE Transactions on Smart Grid*, 3(1):526–534, 2012.

 doi:10.20944/preprints202109.0016.v1